

# Hybrid Membrane based on Polymer-doped Phosposilicate and their Characterization

Uma Thanganathan<sup>1,2,\*</sup>

A class of proton-conducting non-fluorinated hybrid composite membranes was produced based on poly(vinylpyrrolidone)-doped tetraethoxysilicate (TEOS) and triammoniumphosphate ((NH<sub>4</sub>)<sub>3</sub>PO<sub>4</sub>·3H<sub>2</sub>O) with and without phosphoric acid. The formation of hybrid composites was verified by various analyses, such as XRD and <sup>1</sup>H NMR, and the thermal degradation was determined by thermogravimetric analysis. The proton conductivity was measured using impedance spectroscopy and values of 3.4 × 10<sup>-2</sup> S/cm and 2.3 × 10<sup>-2</sup> S/cm were obtained at room temperature for the SiO<sub>2</sub>/P<sub>2</sub>O<sub>5</sub>/(NH<sub>4</sub>)<sub>3</sub>PO<sub>4</sub>/PVP (90/8/2 mol%/1g) and the SiO<sub>2</sub>/(NH<sub>4</sub>)<sub>3</sub>PO<sub>4</sub>/PVP (90/10 mol%/1g) hybrid composite membranes, respectively. The results were discussed based on the effects of P<sub>2</sub>O<sub>5</sub> and (NH<sub>4</sub>)<sub>3</sub>PO<sub>4</sub> on the hybrid composites.

## Introduction

In recent years, the necessity for reducing the pollution, especially in large cities, has attracted more interests on the proton exchange membrane fuel cells (PEMFCs). The main obstacles to commercialization of PEMFCs are largely related to the proton-conducting materials, typically solid polymer electrolytes such as Nafion. This is due to the combined chemical, electrochemical, and mechanical stabilities with high proton conductivity (0.1 S/cm) at ambient temperature of this material [1,2]. However, a profound drawback of Nafion is the low water retention at temperatures above 80 °C. Moreover, these membranes are expensive. A variety of membranes have been developed as alternatives to perfluorosulfonic polymers, such as composites of Nafion and metal oxides [3], sulfonated polymers based on aromatic hydrocarbons [7] and organosiloxane-based inorganic-organic hybrids with various acid species [4].

Organic-inorganic composites have been investigated for PEMFCs with the main objective of increasing the proton conductivity of the membrane [5,6]. The incorporation of highly conductive (0.02 – 0.1 S/cm at room temperature) heteropolyacids such as phosphotungstic acid (PWA) and silicotungstic acid (SiWA) [7] in such composites has shown encouraging results. The inclusion of phosphates into the Nafion

membrane has also exhibited good results. For instance, the addition of zirconium phosphates to Nafion enhanced the water retention characteristics of the membrane at elevated temperatures [8].

Organic-inorganic hybrid materials have shown enhanced stabilities at elevated temperatures and provided high conductivities [9]. Recently, cross-linking between polymer chains containing sulfonic acid was reported to provide proton conductivities three times as large as that of Nafion and to enhance the mechanical stability [10]. Certain studies have been conducted on the research of electrolytes for use at 150–300 °C, and are mainly focused on sulfates, cesium dihydrogen phosphate (CsH<sub>2</sub>PO<sub>4</sub>), and ammonium polyphosphate [11]. It was found that the large conductivity of CsH<sub>2</sub>PO<sub>4</sub> is only achieved in the narrow temperature range between 230 °C and 260 °C. Furthermore, the decrease of the conductivity at 260 °C with an increase of time was also observed [12].

PWA, with a high proton conductivity of about 2 × 10<sup>-1</sup> S/cm at 25 °C [13], was incorporated as a proton source in a silicophosphate amorphous gel structure. According to a study by Park and Nagai [1]. The effect of the acid concentration on glass with PWA or phosphomolybdic acid (PMA) was to yield a high proton conductivity. PWA was successfully used as an electrolyte in H<sub>2</sub>/O<sub>2</sub> fuel cells [14]. Considerable efforts have recently been devoted to NH<sub>4</sub>PO<sub>3</sub>-based electrolytes to enhance conductivity and stability by adding a crystallized supporting matrix, such as SiO<sub>2</sub>, (NH<sub>4</sub>)<sub>2</sub>SiP<sub>4</sub>O<sub>13</sub>, and (NH<sub>4</sub>)<sub>2</sub>Mn(PO<sub>3</sub>) [15].

Recently, Ramya *et. al.* reported on the proton-conducting polymer electrolytes based on poly(vinylpyrrolidone) (PVP)/ammonium thiocyanate (NH<sub>4</sub>SCN) with good thermal and electrical properties [16]. An ammonium polyphosphate (NH<sub>4</sub>PO<sub>3</sub>, APP) composite has recently been introduced to exhibit good conductivities at temperatures of 200–300 °C, especially under wet atmospheres [17,18]. In this composite, APP

<sup>1</sup>Forschungszentrum, GmbH, Institute of Energy and Climate Research, Jülich, Wilhelm-Johnen-Straße, 52428 Jülich, Germany

<sup>2</sup>Research Core for Interdisciplinary Sciences (RCIS), Okayama University, Tsushima-Naka, Kita-Ku, Okayama 700-8530, Japan

\*Corresponding author:

E-mail: ptuma2005@gmail.com (Uma Thanganathan)

Tel.: (+49) 2461 61-85356; Fax: (+49) 2461 61-6695

was responsible for the high ionic conductivity, whereas  $(\text{NH}_4)_2\text{SiP}_4\text{O}_{13}$  served as the supporting matrix. At 250 °C, the conductivity of APP/ $(\text{NH}_4)_2\text{SiP}_4\text{O}_{13}$  was found to be 0.018 S/cm in dry hydrogen and 0.080 S/cm in humidified hydrogen. Stimming *et. al.* [19] announced conductivity values of APP composites up to 0.1 S/cm at 300 °C in a water-rich environment. Moreover, a fuel cell with APP/ $(\text{NH}_4)_2\text{SiP}_4\text{O}_{13}$  as an electrolyte showed a power density of 6.6 mW/cm at 250 °C. These results indicate that the increase in conductivity under humidified conditions may originate from the water that is absorbed into the composite, which participates in the proton conducting by hydrogen bond formation between water and  $[\text{PO}_4]$  tetrahedron [20].

As a water-soluble polymer, PVP has a beneficial effect on protection, viscosity, absorbency, and solubilization, with its most significant features being excellent solubility and biocompatibility. Recently, a great interest has been devoted to the synthesis, characterization and swelling studies of PVP-based hydrogels [21]. Considering the film-forming property of PVP, it was blended with pectin to improve its mechanical properties. PVP is one of the ideal prepolymerized materials owing to its solubility in polar solvents and thermal cross-linking characteristics. Some studies have focused on PVP-based electrolytes for their possible applications in the electrochemical devices [22]. The ionic conduction in polymer electrolytes is dominated by the amorphous rather than the crystalline phase. To enhance the conductivity, several approaches have been suggested [23].

The sol-gel process involves two principal reactions consisting of (i) the hydrolysis of alkoxide groups to form silanol groups, and (ii) the subsequent condensation of silanol groups to produce siloxane bonds in alcohol/water solutions [24]. Hybrid membranes are highly homogenous sols that are usually prepared by the sol-gel process. Many hybrid materials synthesis procedures are based on hydrolysis and condensation reactions of silanes by the sol-gel route [25]. The organically modified silicates present different physical characteristics depending on their chemical composition and the synthetic conditions [26]. The sol-gel technology makes it possible to incorporate organic molecules into an inorganic network, so that they can be combined virtually at any ratio on the molecular level with the formation of hybrid organic-inorganic nanocomposite materials [27].

In this work, hybrid materials were synthesized through sol-gel processes with both commercially and scientifically interest because of their unique properties originating from their hybrid nature. Large proton conductivity was found at room temperature. The investigation enhanced our understanding of non-perfluorinated polymer blended materials and the high ionic conductivity of ammoniumphosphate in the hybrid networks. The properties of this new class of hybrid composite membrane were characterized and compared with those of  $\text{P}_2\text{O}_5$  mixed with ammoniumphosphate and PVP/ $\text{SiO}_2$  membranes.

## Experimental

All chemicals were obtained from Japan and used as received.  $\text{Si}(\text{OC}_2\text{H}_5)_4$  (TEOS, 99.9%, Colcote, Japan), phosphoric acid (Nacalai Tesque, Japan), poly(vinylpyrrolidone) with a molecular weight of 100,000 g/mol (Nacalai Tesque, Japan), and triammonium phosphate trihydrate  $(\text{NH}_4)_3\text{PO}_4 \cdot 3\text{H}_2\text{O}$  (Cica-reagent, Kanto Chemical Co, Japan) were used.

The hybrid composites were prepared in 2 stages: Initially, the starting material of TEOS was hydrolyzed in an acid mixture of ethanol and water ( $\text{C}_2\text{H}_5\text{OH}:\text{H}_2\text{O}$ , 1M HCl, 1:5 ratio) under magnetic stirring at room temperature. Then, trimethyl phosphate was added dropwise to the mixed solution. Next, triammonium phosphate was added to the solution and continuously stirred for 1 h. The total solution was stirred for 8 h under the slow speed of the reaction. In the second stage, PVP was dissolved in water at room temperature and then added to the above mixed solution. The organic part of composite (PVP) was mixed smoothly under stirring and a transparent solution was obtained. This solution was stirred for 24 h at room temperature, which led to the production of a homogenous transparent solution. A homogeneous solution has necessarily a uniform composition with a low scattering loss. The final solution was allowed to dry at room temperature to form a composite, after which the water and heat treatments at 150 and 120 °C were applied for 24 and 12 h, respectively. Subsequently, the final composite membranes were ground to prepare a fine powder for the characterizations with XRD,  $^1\text{H}$  NMR, TGA and conductivity examinations. The thickness of the membrane was in the range of 0.08 – 0.3 mm for the conductivity measurement. Gold electrodes with a 0.2 mm diameter were sputtered onto the composite membranes before the measurements.

The structures of the hybrid composites were characterized using XRD with an X-ray diffraction machine (Rigaku, Multiflex, Japan) with  $\text{CuK}\alpha$  radiation. The range of the diffraction angle  $2\theta$  was 5–60°.  $^1\text{H}$  MAS NMR spectra were recorded on a Varian UNITY1 NOVA300 FT-NMR (Fourier-transform NMR) spectrometer. The thermal stabilities of the hybrid composites were characterized using of thermogravimetric analysis (TGA) techniques. It was carried out on a DTG-50, Shimadzu instrument, performing simultaneous DTA-TG from room temperature to 600 °C at a heating rate of 10 °C/min under nitrogen. The sample masses were kept between 2 and 3 mg. The onset of degradation and the weight loss at 600 °C were evaluated. Impedance spectroscopy studies were carried out on a Solartron, SI-1260 (impedance analyzer), where evaporated-platinum electrodes were used. The conductivity of the membranes was calculated from complex impedance plots in the frequency range from 1 Hz to 1 MHz. The samples were kept in open atmosphere at room temperature during the impedance measurements.

## Results and discussion

The XRD patterns of the composites show the phase information of pure PVP, SiO<sub>2</sub>/P<sub>2</sub>O<sub>5</sub>/(NH<sub>4</sub>)<sub>3</sub>PO<sub>4</sub>/PVP and SiO<sub>2</sub>/(NH<sub>4</sub>)<sub>3</sub>PO<sub>4</sub>/PVP hybrid composite membranes (**Fig. 1(I)**). The broad peaks between  $2\theta = 12^\circ$  and  $22^\circ$  can be associated with the amorphous nature of pure PVP (**Fig. 1(II)**) [28]. Similarly, the broad peaks between  $17^\circ - 28^\circ$  can be associated with the amorphous nature of the composites (**Fig. 1(IIa-d)**). When compared with the pure PVP, a decrease in the relative intensity with broadening of the apparent peak of the SiO<sub>2</sub>/P<sub>2</sub>O<sub>5</sub>/(NH<sub>4</sub>)<sub>3</sub>PO<sub>4</sub>/PVP hybrid composites was observed. This result can be interpreted by considering the reported criterion [29], which establishes a correlation between the intensity of the peak and the degree of crystallinity. However, the phosphosilicate-doped polymer membranes showed the formation of an amorphous phase. The interaction between the salt and polymer caused a decreasing of the crystallinity leading to an amorphous-rich phase, which was manifested by the broad diffraction peak centered at  $2\theta = 18^\circ - 25^\circ$ .

From **Fig. 1(III)**, one can observe the intensity of the peaks at  $16^\circ$ ,  $24^\circ$ ,  $29^\circ$ ,  $33^\circ$ , and  $45^\circ$  in the SiO<sub>2</sub>/(NH<sub>4</sub>)<sub>3</sub>PO<sub>4</sub>/PVP hybrid composite membrane. The intensity of peaks at  $33^\circ$  and  $45^\circ$  disappeared with the increase of SiO<sub>2</sub> (90%) concentration in the composite. Furthermore, the intensity of the main sharp peaks  $2\theta = 16^\circ$ ,  $24^\circ$ , and  $29^\circ$  decreased as the concentration of SiO<sub>2</sub> increased (60 – 90 mol%) and as the amount of (NH<sub>4</sub>)<sub>3</sub>PO<sub>4</sub> decreased (40–10 mol%) in the SiO<sub>2</sub>/(NH<sub>4</sub>)<sub>3</sub>PO<sub>4</sub>/PVP composite membranes (**Fig. 1(IIIa-d)**). From the above observations, the presence of P<sub>2</sub>O<sub>5</sub> with SiO<sub>2</sub> in the hybrid composites was demonstrated by the presence of an amorphous phase (**Fig. 1(II)**), whereas without P<sub>2</sub>O<sub>5</sub> in the hybrid composite, there existed the crystalline peaks.

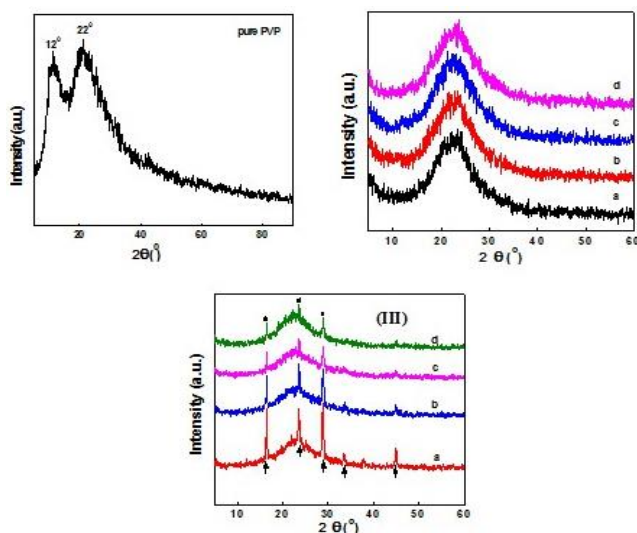


**Fig. 1.** XRD patterns of the (I) pure PVP; (II) SiO<sub>2</sub>/P<sub>2</sub>O<sub>5</sub>/(NH<sub>4</sub>)<sub>3</sub>PO<sub>4</sub>/PVP hybrid composite: (a) 90/2/8 (mol%)/1 g, (b) 90/4/6 (mol%)/1 g, (c) 90/6/4 (mol%)/1 g and (d) 90/8/2 (mol%)/1 g; (III) the SiO<sub>2</sub>/(NH<sub>4</sub>)<sub>3</sub>PO<sub>4</sub>/PVP hybrid composite: (a) 60/40 (mol%)/1 g, (b) 70/30 (mol%)/1 g, (c) 80/20 (mol%)/1 g, and (d) 90/10 (mol%)/1 g.

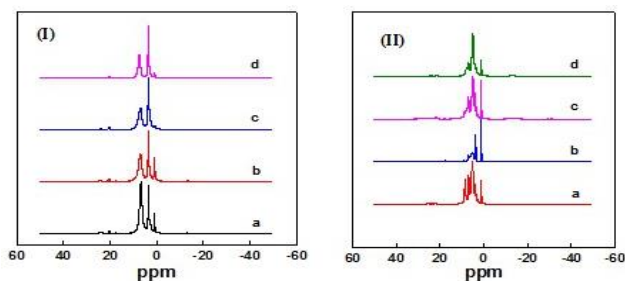


**Fig. 2.** <sup>1</sup>H NMR spectra of the (I) SiO<sub>2</sub>/P<sub>2</sub>O<sub>5</sub>/(NH<sub>4</sub>)<sub>3</sub>PO<sub>4</sub>/PVP hybrid composite: (a) 90/2/8 (mol%)/1 g, (b) 90/4/6 (mol%)/1 g, (c) 90/6/4 (mol%)/1 g, (d) 90/8/2 (mol%)/1 g; (II) SiO<sub>2</sub>/(NH<sub>4</sub>)<sub>3</sub>PO<sub>4</sub>/PVP hybrid composite: (a) 60/40 (mol%)/1 g, (b) 70/30 (mol%)/1 g, (c) 80/20 (mol%)/1 g, (d) 90/10 (mol%)/1 g.

**Fig. 2** displays the <sup>1</sup>H NMR spectra for the SiO<sub>2</sub>/P<sub>2</sub>O<sub>5</sub>/(NH<sub>4</sub>)<sub>3</sub>PO<sub>4</sub>/PVP and SiO<sub>2</sub>/(NH<sub>4</sub>)<sub>3</sub>PO<sub>4</sub>/PVP hybrid composite membranes. In **Fig. 2(I and II)**, the peak resonance positions had the same chemical shift anisotropies as observed in the composites, mainly for the peaks at 8.1, 5.1, and 1.1 ppm (**Fig. 2(I)**); and at 7.1, 4, and 1.1 ppm (**Fig. 2(II)**). The chain length dramatically decreased to 8.1 and 7.1 ppm; the center peaks at 5.1 and 4 ppm did not go through any changes even after altering the chemical concentration. The PVP/SiO<sub>2</sub> hybrid material had C=O absorption peaks at 8.1 and 7.1 ppm as shown in **Fig. 2(I and II)**.

It was clearly noted that three units decreased or increased, and these changes depended on the amounts of P<sub>2</sub>O<sub>5</sub> (2, 4, 6, and 8 mol%) and (NH<sub>4</sub>)<sub>3</sub>PO<sub>4</sub> (8, 6, 4, and 2 mol%) in the SiO<sub>2</sub>/P<sub>2</sub>O<sub>5</sub>/(NH<sub>4</sub>)<sub>3</sub>PO<sub>4</sub>/PVP hybrid composite membrane. When the concentration of P<sub>2</sub>O<sub>5</sub> increased and the amount of (NH<sub>4</sub>)<sub>3</sub>PO<sub>4</sub> decreased, the peaks at 8.1 and 1.1 ppm decreased and no significant changes were noted for the center peak at 5.1 ppm (**Fig. 2(I)**). In the <sup>1</sup>H NMR spectra of the SiO<sub>2</sub>/(NH<sub>4</sub>)<sub>3</sub>PO<sub>4</sub>/PVP hybrid composite membranes, the center peak at 4 ppm did not show significant changes for any of the samples, and the peak at 1.1 ppm decreased as the amount of SiO<sub>2</sub> increased and the amount of (NH<sub>4</sub>)<sub>3</sub>PO<sub>4</sub> decreased.

This result indicates that there were hydrogen bonds between the >C=O group in PVP and SiO<sub>2</sub> in the inorganic phase. Furthermore, the greater the amount of TEOS, the more the peak shifted up field, although this may be not sufficient to indicate the presence of a hydrogen bond between PVP and SiO<sub>2</sub>. However, some studies have reported that hydrogen bonding does take place between the C=O in PVP and the OH in SiO<sub>2</sub> [30].

The TGA thermograms of the SiO<sub>2</sub>/P<sub>2</sub>O<sub>5</sub>/(NH<sub>4</sub>)<sub>3</sub>PO<sub>4</sub>/PVP and SiO<sub>2</sub>/(NH<sub>4</sub>)<sub>3</sub>PO<sub>4</sub>/PVP hybrid composite membranes are shown in **Fig. 3**. The first weight loss started at 30°C for the SiO<sub>2</sub>/P<sub>2</sub>O<sub>5</sub>/(NH<sub>4</sub>)<sub>3</sub>PO<sub>4</sub>/PVP composites (**Fig. 3(I)**), which was attributed to the loss of water contained in the composites. The second weight loss started at around 200–250 °C and continued up to 450–500 °C. Above 500 °C, there was no dehydration for any of the samples. In **Fig. 3(II)**, the first weight loss took place at 35 °C and

the second weight loss at 190 °C. The latter one was attributed to the decomposition of C=O groups in the PVP main chain. The decomposition temperature shifted by 35 °C as a result of strengthened hydrogen-bonding interactions between PVP and the SiO<sub>2</sub> matrix. Above 350 °C, degradation took place for the SiO<sub>2</sub>/(NH<sub>4</sub>)<sub>3</sub>PO<sub>4</sub>/PVP composite, confirming that this composite was thermally stable up to 200 °C.

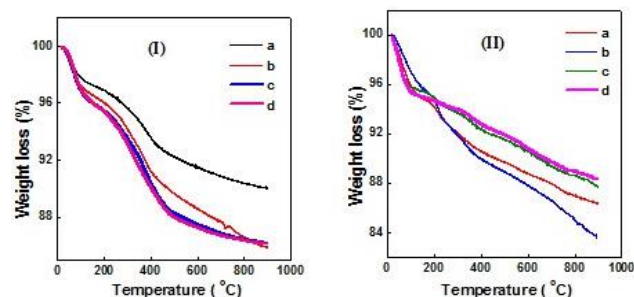


**Fig. 3.** TGA traces for the (I) SiO<sub>2</sub>/P<sub>2</sub>O<sub>5</sub>/(NH<sub>4</sub>)<sub>3</sub>PO<sub>4</sub>/PVP hybrid composite: (a) 90/2/8 (mol%)/1 g, (b) 90/4/6 (mol%)/1 g, (c) 90/6/4 (mol%)/1 g, (d) 90/8/2 (mol%)/1 g; (II) SiO<sub>2</sub>/(NH<sub>4</sub>)<sub>3</sub>PO<sub>4</sub>/PVP hybrid composite: (a) 60/40 (mol%)/1 g, (b) 70/30 (mol%)/1 g, (c) 80/20 (mol%)/1 g, (d) 90/10 (mol%)/1 g.

The initial decomposition temperature and rate decreased as the quantity of TEOS increased. The reason for this phenomenon was that during hydrolysis, Si(OH)<sub>4</sub> was formed by TEOS in the hybrid materials. Later, polymerization took place and SiO<sub>2</sub> was formed, but some of the Si(OH)<sub>4</sub> did not totally complete the process, a phenomenon that becomes more apparent with increasing the amount of TEOS. However, after decomposition of Si(OH)<sub>4</sub>, what remained in the hybrid material was the lattice structure formed by PVP and SiO<sub>2</sub>, causing the decomposition rate to decrease. This also means that the heat resistance of the hybrid material was improved. The thermal analysis confirmed the thermal stability of the SiO<sub>2</sub>/P<sub>2</sub>O<sub>5</sub>/(NH<sub>4</sub>)<sub>3</sub>PO<sub>4</sub>/PVP and SiO<sub>2</sub>/(NH<sub>4</sub>)<sub>3</sub>PO<sub>4</sub>/PVP hybrid composite membranes up to 450 and 200 °C, respectively.

The impedance spectra of the SiO<sub>2</sub>/P<sub>2</sub>O<sub>5</sub>/(NH<sub>4</sub>)<sub>3</sub>PO<sub>4</sub>/PVP hybrid composite membranes are presented in **Figs. 4 and 5**. The conductivities for all the composites were measured at room temperature under an open atmosphere. Before the measurements, all the samples were heated to 100 °C for 1 h in an oven. The impedance spectra at room temperature presented a semicircle and a line, related to the bulk resistance-high frequency arc plus low frequency arc and electrode resistance. The Cole-Cole plot consisted of a single semicircle and the conductivity was obtained from the intersecting point of the semicircle with the real axis. The total resistance of the hybrid membrane, *R*, is thus the sum of *R*<sub>1</sub> and *R*<sub>2</sub> [cf: inside **Figs. 4 and 5**: equivalent circuit]. The impedance consists of well-defined parts (low and high frequency arcs). This semi-circle represents a typical equivalent circuit of a resistor and a capacitor connected in parallel and corresponds to the bulk electrical properties. The resistance *R* was obtained from the intersection of the

semicircle with the Re (*Z'*) axis calculated using fitting software.

The experimental impedance data for the hybrid membranes were analyzed by fitting of the corresponding equivalent circuit. The semicircle can be represented by a parallel combination of a capacitor, which was due to the immobile polymer chain and a resistor due to the resistance offered by the polymer/SiO<sub>2</sub> matrix to the mobile ion. The low frequency arc can be attributed to the effect of blocking electrodes. The low frequency response appearing as an inclined arc was distinctly vertical to both axes.

As expected, a high conductivity from  $1.8 \times 10^{-2}$  to  $3.4 \times 10^{-2}$  S/cm was obtained at room temperature for all composites [**Fig. 4**]. The SiO<sub>2</sub>/P<sub>2</sub>O<sub>5</sub>/(NH<sub>4</sub>)<sub>3</sub>PO<sub>4</sub>/PVP (90/8/2 mol%/1g) composite exhibited the largest conductivity of  $3.4 \times 10^{-2}$  S/cm, and it was clear that the contents of P<sub>2</sub>O<sub>5</sub> (8 mol%) and (NH<sub>4</sub>)<sub>3</sub>PO<sub>4</sub> (2 mol%) and their distribution in the SiO<sub>2</sub>/P<sub>2</sub>O<sub>5</sub>/(NH<sub>4</sub>)<sub>3</sub>PO<sub>4</sub>/PVP hybrid matrix of the membrane played key roles in the proton conduction. The POH group was strongly hydrogen-bonded with the water molecules as opposed to that of the Si-OH groups [31]. Moreover, the proton conductivity of the composite could be enhanced by enriching the concentration of P-OH groups in the PVP/SiO<sub>2</sub> hybrids. As a result of the distribution of triammonium phosphate in the hybrid matrix, the conductivity and stability enhanced. The crystallized supporting matrix, such as SiO<sub>2</sub> and P<sub>2</sub>O<sub>5</sub>, were also responsible for the enhancement [32]. The presence of these phosphorous species was fundamental to the proton conduction process providing protons which could be exchanged by neighboring groups, hydroxyl groups, and adsorbed water to facilitate a Grotthuss proton transport [33]. For the conductivity, both triammonium phosphate and P<sub>2</sub>O<sub>5</sub> were main contributors to the hybrid composite membranes and helped to increase the thermal stability and proton conductivity. According to this study, the presence of P<sub>2</sub>O<sub>5</sub> and (NH<sub>4</sub>)<sub>3</sub>PO<sub>4</sub> in the hybrid composition played a significant role for providing high proton conduction. This topic will be investigated further in the near future.

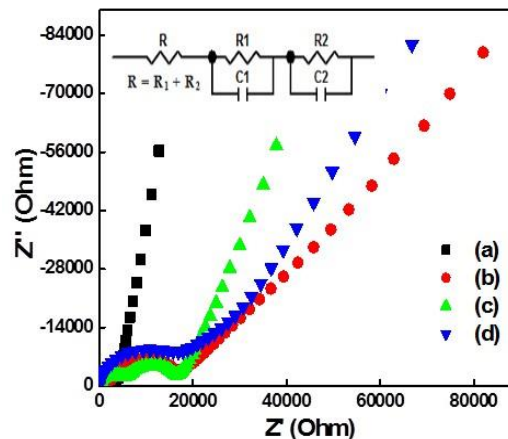


**Fig. 4.** Impedance spectra of SiO<sub>2</sub>/P<sub>2</sub>O<sub>5</sub>/(NH<sub>4</sub>)<sub>3</sub>PO<sub>4</sub>/PVP hybrid composite: (a) 90/2/8 (mol%)/1 g, (b) 90/4/6 (mol%)/1 g, (c) 90/6/4 (mol%)/1 g, (d) 90/8/2 (mol%)/1 g.

Fig. 5 illustrates the proton conductivity of the  $\text{SiO}_2/(\text{NH}_4)_3\text{PO}_4/\text{PVP}$  hybrid composite membrane, which was found in the range from  $1.4 \times 10^{-2}$  to  $2.3 \times 10^{-2}$  S/cm at room temperature. Such values were somewhat lower than those mentioned above (Fig. 4) but remained in the same order of magnitude (i.e.,  $10^{-2}$  S/cm). The content of  $(\text{NH}_4)_3\text{PO}_4$  was the reason for the larger conductivity illustrated in Fig. 5(d) as opposed to the other composites. The semicircle that was observed for these hybrid membranes at high frequencies was no longer present. This behavior suggests a fast ionic transport through the hydrophilic network [34].

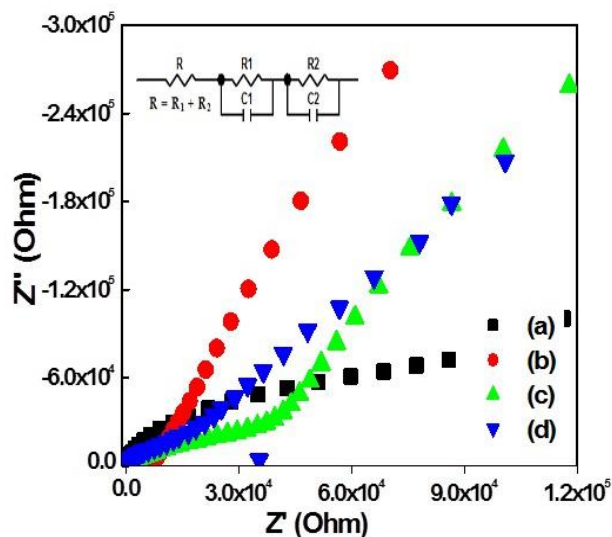


Fig. 5. Impedance spectra of  $\text{SiO}_2/(\text{NH}_4)_3\text{PO}_4/\text{PVP}$  hybrid composite: (a) 60/40 (mol%)/1 g, (b) 70/30 (mol%)/1 g, (c) 80/20 (mol%)/1 g, (d) 90/10 (mol%)/1 g.

At low temperature the translational modes are usually excluded from such dynamics, and the conductivity is of Grotthuss-type [35]. The  $-\text{OH}$  groups on the surface co-ordinated the water molecules, providing alternative hopping paths in the case of a Grotthuss-like transport mechanism [36]. Grotthuss-type mechanisms are more likely to occur than the migration of hydroxyl ions for simple structural reasons [37]. The principal proton conduction mechanism involves proton transfer between adjacent  $\text{OH}^-$  and  $\text{O}_2^-$  and  $\text{OH}$  reorientation (Grotthuss mechanism) rather than  $\text{OH}$  diffusion, as sometimes is emphasized [38]. There are two possible mechanisms that govern the proton transport in the proton-conducting membrane, one involving structural diffusion, known as the Grotthuss mechanism and the other one involving a vehicle-style migration [39]. In the Grotthuss mechanism, proton transfer occurs between protogenic groups followed by a reorganization of hydrogen bonds. In the vehicle mechanism, the protons are transported in a diffusion-style process with the aid of carriers such as water in the form of  $\text{H}_3\text{O}^+$ . The most trivial case of proton migration requires the translational dynamics of bigger species, which is the vehicle mechanism [40]. In this mechanism the proton diffuses through the medium

together with a vehicle (for example, with  $\text{H}_2\text{O}$  as  $\text{H}_3\text{O}^+$ ). The counter diffusion of unprotonated vehicles ( $\text{H}_2\text{O}$ ) allows the net transport of protons.

The conductivity values mentioned above were greater than those recently reported for a  $\text{NH}_4\text{PO}_3/\text{SiO}_2/\text{P}_2\text{O}_5$  glass proton conductor, which showed a total conductivity of 6.0–19 mS/cm in the temperature range of 150–250 °C, for intermediate temperature fuel cells. Furthermore, the proton conductivities of the present hybrid composite membranes were also compared with the results from a similar study of proton conductivity on hybrid membranes for low and high temperature fuel cells [41].

## Conclusions

High proton-conducting hybrid composite membranes were successfully fabricated and their structural and proton conductivity properties were studied. Analysis by XRD,  $^1\text{H}$  NMR, and TGA confirmed that the composites were homogeneously formed by the sol-gel method. The XRD patterns of both the hybrid composite membranes indicated that the amorphous phase of the polymer increased as the  $\text{SiO}_2$  concentration was raised. From the TGA examinations, it was found that the presence of  $\text{SiO}_2$  network was responsible for the greater thermal stability of these hybrid membranes. High proton conductivities of  $3.4 \times 10^{-2}$  S/cm and  $2.3 \times 10^{-2}$  S/cm were obtained for the  $\text{SiO}_2/\text{P}_2\text{O}_5/(\text{NH}_4)_3\text{PO}_4/\text{PVP}$  (90/8/2 mol%/1g) and  $\text{SiO}_2/(\text{NH}_4)_3\text{PO}_4/\text{PVP}$  (90/10 mol%/1g) hybrid composite membranes at room temperature, respectively. The studies revealed promising materials for applications in fuel cells and suitable electrolytes for low/intermediate temperature fuel cells.

## Acknowledgements

The author thanks the Alexander von Humboldt Foundation (AvH), for giving opportunity to stay in Germany. This work was supported by a grant of the Japan Science and Technology (JST), Japan.

## Keywords

Hybrid materials, composites, fabrication, membranes.

Received: 6 November 2020

Revised: 20 January 2021

Accepted: 13 February 2021

## References

- Park, Y.; Nagai, M.; *J. Electrochem. Soc.*, **2001**, *148*, A616.
- Kato, M.; Katayama, S.; Sakamoto, W.; Yogo, T.; *Electrochim. Acta.*, **2007**, *52*, 5924.
- Adjemian, K. T.; Dominey, R.; Krishnan, L.; Ota, H.; Majstrik, P.; Zhang, T.; Mann, J.; Kirby, B.; Gatto, L.; Velo-Simpson, M.; Leahy, J.; Srinivasant, S.; Benziger, J.B.; Bocarsly, A.B.; *Chem. Mater.*, **2006**, *18*, 2238.
- Xing, P.X.; Robertson, G.P.; Guiver, M.D.; Mikhailenko, S.D.; Wang, K.P.; Kaliaguine, S.; *J. Membrane Sci.*, **2004**, *229*, 95.
- Vernon, D.R.; Meng, F.Q.; Dec, S.F.; Williamson, D.L.; Turner, J.A.; Herring, A.M.; *J. Power Sources.*, **2005**, *139*, 141.
- Kim, Y.M.; Choi, S.H.; Lee, H.C.; Hong, M.Z.; Kim, K.; Lee, H.I.; *Electrochim. Acta.*, **2004**, *49*, 4787.
- Shao, Z. G.; Joghee, P.; Hsing, I.M.; *J. Membr. Sci.*, **2004**, *229*, 43.
- Kim, Y.T.; Song, M.K.; Kim, K.H.; Park, S.B.; Min, S.K.; Rhee, H.W.; *Electrochim. Acta.*, **2004**, *50*, 645.

9. Lee, S.Y.; Scharfenberger, G.; Meyer, W.H.; Wegner, G.; *Adv. Mater.*, **2005**, *17*, 626.
10. Service, R.F.; *Science.*, **2006**, *312*, 35.
11. Yan, W.M.; Chu, H.S.; Lu, M.X.; Weng, F.B.; Jung, G.B.; Lee, C.Y.; *J. Power Sources*, **2009**, *188*, 141.
12. Boysen, D.A.; Haile, S.M.; *Chem. Mater.*, **2003**, *15*, 727.
13. Maruyama, T.; Saito, Y.; Matsumoto, Y.; Yano, Y.; *Solid State Ionics.*, **1985**, *17*, 281.
14. Uma, T.; Nogami, M.; *Fuel Cells.*, **2007**, *4*, 279.
15. Chen, X.; Li, X.; Jiang, S.; Xia, C.; Stimming, U.; *Electrochim. Acta.*, **2006**, *51*, 6542.
16. Cappadonia, M.; Niemzigand, O.; Stimming, U.; *Solid State Ionics.*, **1999**, *125*, 333.
17. Ramya, C.S.; Selvasekarapandian, S.; Savitha, T.; *J. Solid State Electrochem.*, **2008**, *12*, 807.
18. Ramya, C.S.; Selvasekarapandian, S.; Savitha, T.; Hirankumar, G.; Angelo, P.C.; *Physica.B.*, **2007**, *393*, 11.
19. Uma, T.; Tu, H.Y.; Freude, D.; Schneider, D.; Stimming, U.; *J. Mater. Sci.*, **2005**, *40*, 227.
20. Matsui, T.; Takeshita, S.; Iriyama, Y.; Abe, T.; Ogumi, Z.; *J. Electrochem. Soc.*, **2005**, *152*, A167.
21. Zhang, X.; Takegoshi, K.; Hikichi, K.; *Macromolecules.*, **1992**, *25*, 2336.
22. Giordano, N.; Staiti, P.; Hocevar, S.; Arico, A.S.; *Electrochim. Acta.*, **1996**, *41*, 397.
23. Sun, C.W.; Stimming, U.; *Electrochim. Acta.*, **2008**, *53*, 6417.
24. Yang, C.C.; Lin, S.J.; Hsu, S.T.; *J. Power Sources.*, **2003**, *122*, 210.
25. Song, Y.; Fenton, J.M.; Kunz, H.R.; Bonville, L.J.; Williams, M.V.; *J. Electrochem. Soc.*, **2005**, *152*, A539.
26. Schuster, M.; Rager, T.; Noda, A.; Kreuer, K.D.; Maier, J.; *Fuel Cells.*, **2005**, *5*, 355.
27. Szu, S.P.; Klein, L.C.; Greenblatt, M.; *J. Non-Cryst. Solids.*, **1992**, *143*, 21.
28. Mackenzie, J.D.; Bescher, E.; *J. Sol-Gel Sci. Technol.*, **2003**, *26*, 7.
29. Hodge, R.M.; Edward, G.H.; Simon, G.P.; *Polymer.*, **1996**, *37*, 1371.
30. Chen, X.; Huang, Z.; Xia, C.; *Solid State Ionics*, **2006**, *177*, 2413.
31. Goncharuk, E.V.; Pakhovchishin, S.V.; Zarko, V.I.; Gun'ko, V.M.; *Colloid J.*, **2001**, *63*, 283.
32. So, S.Y.; Kim, S.C.; Lee, S.Y.; *J. Membr. Sci.*, **2010**, *360*, 210.
33. Jiang, Y.; Matthieu, T.; Lan, R.; Xu, X.; Cowin, P.I.; Tao, S.; *Solid State Ionics.*, **2011**, *192*, 108.
34. Slade, S.; Campbell, S.A.; Ralph, T.R.; Walsh, F.C.; *J. Electrochem. Soc.*, **2002**, *149*, A1556.
35. Li, S.; Liu, M.; *Electrochim. Acta.*, **2003**, *48*, 4271.
36. Clearfield, A.; *J. Mol. Catal.*, **1988**, *88*, 125.
37. Kopitzke, R.W.; Linkous, C.A.; Anderson, H.R.; Nelson, G.L.; *J. Electrochem. Soc.*, **2000**, *147*, 1677.
38. Kreuer, K.D.; Schonherr, E.; Maier, J.; *Solid State Ionics.*, **1994**, *278*, 70.
39. Iwahara, H.; Uchida, H.; Morimoto, K.; *J. Electrochem. Soc.*, **1990**, *137*, 462.
40. Kreuer, K.D.; Rabenau, A.; Weppner, W.; *Angew. Chem.*, **1982**, *94*, 224.
41. Tung, S.P.; Hwang, B.J.; *Fuel Cells.*, **2007**, *7*, 32.